УДК 620.91

SOLID OXIDE FUEL CELL STACK OPTIMIZATION USING MULTI-PHYSICS NUMERICAL MODEL

A.U. Sharafutdinov[1], Yu.S. Fedotov[1], S.I. Bredikhin[1]

[1]*Institute of Solid State Physics RAS, 142432, Russia, Chernogolovka, Moscow region, Academician Ossipyan, 2,*

e-mail: shazat@issp.ac.ru

NiO/10Sc1CeSZ/LSM membrane-electrode assembly (MEA) was prepared using screen printing technology. A series of current-voltage characteristics was measured. Using experimental data a numerical model of SOFC stack was composed in COMSOL Multiphysics finite element analysis software. Distributions of temperature, reactants concentrations, gas pressures and velocities were calculated. It was found that high heat exchange efficiency in gas distribution domains of the stack suppresses the dependence of temperature variation amplitude in the reaction zone on the temperature of input airflow. This allows to lower the rate of input airflow avoiding significant growth of temperature gradients across the stack. It was also shown that the main pressure drop on the stack is due to generation of vortices in the input manifold and not to laminar flow losses.

***Keywords**: SOFC, COMSOL, electrolyte-supported cell, fuel cell stack, computational fluid dynamics*

INTRODUCTION

During the past decades the developed countries have made many efforts to reduce the percentage of traditional energy sources in overall energy balance as well as to increase the energy efficiency. The reasons lie in growing energy demands together with finiteness of fuel deposits: newly discovered volumes cannot level with the consumption rates. Besides their development complexity and costs grow rapidly. The environmental health aspect has the same degree of importance. The tendency for the “green” economy is quite strong and is manifested in different industries. In automotive it is seen as gradual ban of diesel engines and rise of electric and hybrid vehicles [1]. In energetics it is growth of smart greed solutions and shift to distributed renewable energy production. Japan has started an ambitious project of transition to the “hydrogen society” by 2020 [2].

Solid oxide fuel cells technology has a great potential due to high energy efficiency and purity compared to traditional ones. It bases on the galvanic process, in which the electrolyte is solid,

conducts only O^{2-} and forms a membrane between the oxidizer, typically air, from the one side and fuel gas from the other side. The process at the electrodes takes place as long as air and fuel gas are separately fed to the cell. As a result the cell produces the electrical energy, heat, steam and CO_2. The working temperature of such devices varies in the range 600–900°C based on the materials and structure used [3]. As for the fuel, it may be either pure hydrogen or syngas, a product of hydrocarbons complete or partial reforming, containing H_2, CO and certain amounts of CH_4. Electrochemical fuel oxidation does not lead to formation of poisonous nitrogen oxides at these temperatures in contrast with conventional fuel burning. The efficiency of the cell is limited not by the Carnot cycle but by the oxidation Gibbs free energy divided by the heat of combustion [4]. Hence, the energy efficiency for natural gas can potentially reach 70% which is extremely rewarding.

The fuel cell always contains three main parts: electrolyte membrane and two electrodes, anode at the fuel side and cathode at the air side. Therefore, the cell is often named membrane-electrode assembly (MEA) to distinguish certain item from the technology name. The typical operating voltage of a cell is 0.7–0.8 V, typical current density 0.2–1 A/cm^2. MEAs differ in geometry and mechanical support. The main geometry types are planar and tubular [5] while the supporting role may be assigned for either the electrolyte membrane, anode, cathode or special external layer [6]. In this paper we focus on the planar electrolyte-supported cells (ESC) since they are developed in ISSP RAS. The sizes of planar MEAs, which can be found in industry, are usually not far from 10x10 cm. MEA thickness varies from 0.12-0.15 mm for the ESC design to about 1 mm for other support types.

For energy production the MEAs are stacked together by 20–60 pieces. It leads to multiplying the voltage up to values suitable for practical use.

PURPOSE OF THE ARTICLE

During the operation of the SOFC a lot of phenomena take place: electrochemical reactions, transport of mass, charge and heat. Each transport phenomenon induces a problem, which should be solved for obtaining the corresponding flux distribution. But they are not independent. Reaction thermodynamics strongly depends on the gas species concentration which in turn hinges on the reaction rate. The heat is produced by electric currents and reactions and drown by gas flows. Almost all important properties depend on the temperature: electric and heat conductivity, density, viscosity, reaction kinetics, etc. For the SOFC system in general case those three transport problems should be solved simultaneously in close connection which makes the analytical approach practically impossible.

Meanwhile the accurate solution is in demand, because the temperature distribution makes strong influence on degradation processes, mechanical stresses, overall stack efficiency [7]. It is important to keep temperature gradients low to increase lifetime of fuel cells and avoid cracks formation. The experimental investigation needs many efforts, funding, and is greatly complicated by high temperatures and sealing obligations. Thus, the best choice for the stack optimization is verified computational model [8].

EXPERIMENTAL PART

Electrolyte-supported MEA was made by electrode deposition on ceramic electrolyte plate using screen printing technique. Plates of ceramic electrolyte were prepared in the following sequence: 1) preparation of ceramic slurry 2) ceramic tape casting 3) tape drying 4) lamination of stacks 5) removing bundles 6) sintering [9]. Electrolyte gains mechanical stability during the sintering process at 1500 ºC. At this temperature the density of resulting electrolyte is maximal. Chemical composition of electrolyte was as follows: 10%Sc_2O_3 1%CeO_2 89%ZrO_2, the thickness was 250 μm. Anode and cathode were deposited by screen printing technique followed by sintering.

HERAEUS V-006 was used as binder for screen printing pastes. Both electrodes were build in two layers: functional and current collection layer. Anode functional layer of 15 μm thickness consisted of 40 wt.% NiO and 60 wt.% 10Sc1CeSZ. Anode current collector layer (ACCL) of 30 μm thickness contained 60 wt.% NiO and 40 wt.% 10Sc1CeSZ. After anode deposition the plate was fired at 1380 ºC. Then cathode was deposited. Cathode functional layer of 15 μm thickness contained 60 wt.% $(La_{0.8}Sr_{0.2})_{0.95}MnO_3$ and 40 wt.% 10Sc1CeSZ. Cathode current collector layer (CCCL) of 30 μm thickness was consisted pure $(La_{0.8}Sr_{0.2})_{0.95}MnO_3$. After cathode deposition the plate was fired at 1100 ºC.

Current-voltage characteristics were measured on a button cell of 21 mm diameter.

Four-probe method was applied for the measurement using potentiostat/galvanostat. Platinum mesh and wiring were used to connect MEA to potentiostat/galvanostat [10]. Air and fuel flow rates were high enough to assume uniform concentrations of chemical species across the button cell surface.

Aforementioned characteristics provide us enough information on electrochemical transport to build a numerical model of the fuel cells stack based on this MEA.

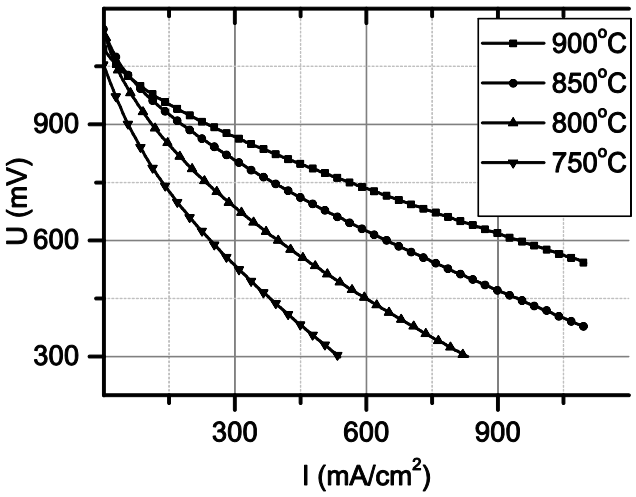

Fig. 1 Current voltage characteristics of ESC.

NUMERICAL MODEL

Nomenclature

R	Universal gas constant
F	Faradey constant
T	Temperature
$\vec{q}$	Heat flow
j	Density of electronic current
$\vec{u}_g$	Effective gas flow speed (here and further index g stands for air or fuel)
ρ_g	Density of gas g
μ_g	Dynamic viscosity of gas g
p_i	Pressure of gas specie i
h_l	Height of layer corresponding to one SOFC in stack
$\mathbf{k}_p$	Thermal conductivity matrix of effective body

1. Geometric setup

The model is composed in COMSOL Multiphysics finite-element analysis software [11] based on the stack design of a prototype crossflow SOFC, which is being developed in ISSP RAS. Model consists of SOFC stack, air and fuel supply pipes and thermal insulation.

Stack includes of 34 MEAs alternated with Crofer 22APU steel interconnects (**Fig. 2**) and high-temperature glass-ceramic sealing compound [12]. Stack is compressed between two thick 20 mm Crofer 22APU steel plates to ensure sealing.

Reactants reach the MEA electrodes through the channels milled on the plates surface. The channels width is small enough to assume lossless current collection (**Table 1**).

We do not define the channels explicitly in our model to reduce computational effort. Instead, we divide our stack into virtual media domains accounting layered structure by effective parameters such as porosity, anisotropic thermal and electric conductivities etc.

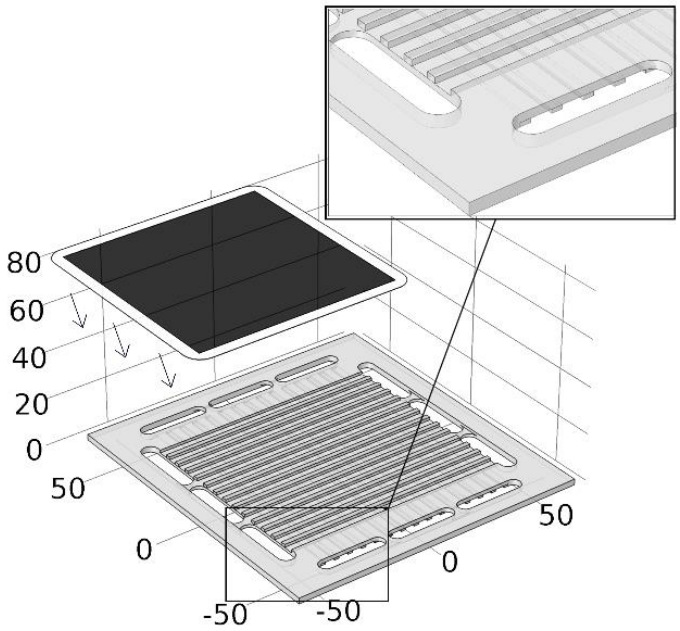

Fig. 2 Membrane electrode assembly and interconnect plate. Width and depth of channels are doubled for visualization. All dimensions are in millimeters.

Table 1 Dimensions of key components of the reaction zone

Stack component	Thickness/Width
Glass-ceramic sealing	150 μm
Steel interconnect	2,3 mm
Electrolyte membrane	250 μm
Electrodes	45 μm
Air channels	0,8 mm/2 mm
Fuel channels	0,4 mm/2 mm

Thus, we have virtual media of six types: 1 – reaction zone; 2 – gas distributor; 3 – stiffening bridges; 4 – outer frame; 5 – end plates (**Fig. 3**); 6 – air and fuel supply manifolds (not displayed).

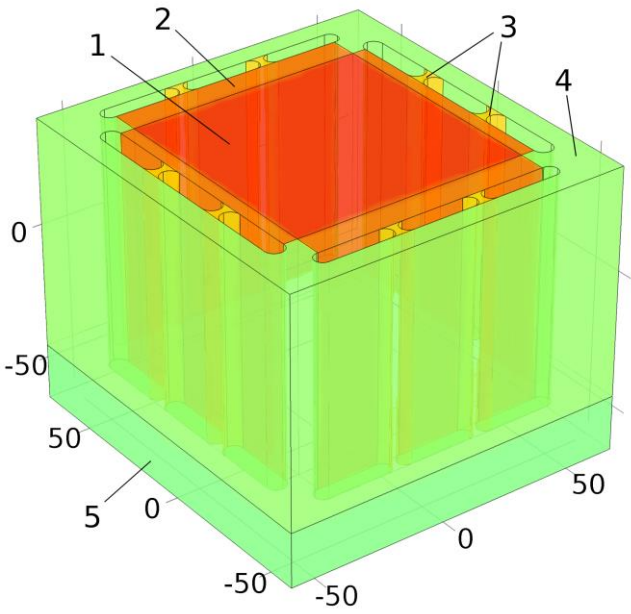

Fig. 3 Stack with domains of various virtual media denoted. All dimensions are in millimeters.

Air and fuel supply lines were assumed to be welded to the upper end plate (see **Fig. 4**). Parameters of 50 mm-thick PROMALIGHT-1000X was used to model thermal insulation.

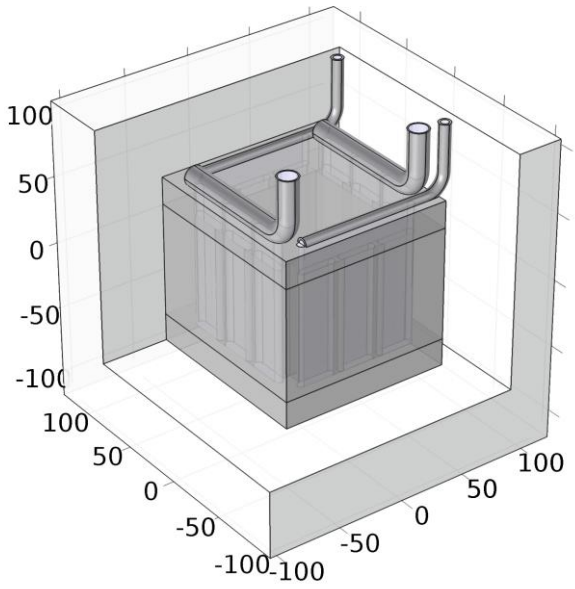

Fig. 4 Outline of full model. Part of insulation is hidden. All dimensions are in millimeters.

2. Physical model

A. Heat transfer

Temperature distribution is given by heat equation in porous media:

$$\sum_g \rho_g C_p^g \vec{u}_g \cdot \nabla T + \nabla \cdot \vec{q} = Q_V$$

$$\vec{q} = -\mathbf{k}_p \nabla T$$

Here summation (index g) runs over gases flowing through the media – air or fuel. Q_V stands for heat dissipation due to thermal effect of reaction and ohmic heating. C_p^g is specific heat of gas flowing through the channels.

Thermal yield of hydrogen oxidation reaction is proportional to the current density in MEA and entropy change during reaction:

$$Q_r = -\frac{j}{2F} T\Delta S \equiv j * U_q$$

Using tabulated values of entropy change during hydrogen oxidation, values of U_q was found at 1000 K, 1100 K и 1200 K. Then we approximated U_q by following linear function:

$$U_q = -0{,}0282 + 3{,}15 * 10^{-4} * T - \frac{RT}{2F} ln\left(\frac{p_{H_2}}{p_{H_2O}} \sqrt{\frac{p_{O_2}}{p_0}}\right)$$

Specific heat of gas mixtures were calculated as average specific heat of components with mass fractions as weights. One can neglect heat conductivity of gases in porous media, in comparison to that of steel. Heat conductivity matrix $\mathbf{k}_p$ is anisotropic in virtual media 1,2,3 and 4 due to laminated structure of stack and presence of gas channels (**Table 2**).

Table 2 Components of thermal conductivity matrix ($\frac{W}{m \cdot K}$) at 780 ºC.

	$\mathbf{k}_p^{xx}$	$\mathbf{k}_p^{yy}$	$\mathbf{k}_p^{zz}$
Reaction zone	14,8	13,5	9,0
Air distribu-tor	18,3	16,0	8,5
Fuel distribu-tor	19,5	20,4	9,6
Stiffening bridges (air)	16,1	16,1	0,1
Stiffening bridges (fuel)	20,0	20,0	0,1
Outer frame	23,9	23,9	10,9

Surface-to-surface radiative heat transfer was accounted for within the manifolds.

B. Charge transfer

Distribution of electric current is given by charge conservation law

$$\nabla \cdot j = 0,$$

and electrochemical transport equations with anisotropic conductivity matrix:

$$j = -\sigma \frac{\nabla \tilde{\mu}}{z_{O^{2-}}} = -\sigma(\nabla \varphi + \frac{U_{rev}}{h_l})$$

Here $\nabla\tilde{\mu}$ is electrochemical potential [13], $z_{O^{2-}}$ is charge of O^{2-} ion ($= -2e$), U_{rev} is output voltage of single SOFC in open circuit regime. U_{rev} is defined by local temperature and concentrations of reactants.

Conductivity depends on the value of electric field nonlinearly. We obtained this dependence from experimental current-voltage characteristics (see **Fig. 1**). Using following approximation functions

$$i = \frac{U}{B + Ae^{-\frac{U}{b}}}$$

current-voltage characteristics could be fitted accurately. Here *A*, *B* and *b* are fitting parameters and depend on temperature (see **Table 3**).

Table 3 Fitting parameters of current-voltage characteristics

	800°C	850°C	900°C
A	2,87584	2,08166	1,29107
b	0,33113	0,23256	0,1548
B	0,54941	0,48132	0,37532

C. Transfer of chemical species.

Equations stated in next two sections are gas-specific, index g is omitted for brevity.

Fuel is mixture of H_2 and H_2O and air is approximated as mixture of N_2 and O_2. To find the evolution of gas mixtures chemical composition across the stack the following equations was used:

$$\nabla \cdot \vec{J_i} + \rho(\vec{u} \cdot \nabla)\omega_i = 0$$

$$\vec{J_i} = -\rho\omega_i \sum_k D_{ik}\overrightarrow{d_k}$$

$$\overrightarrow{d_k} = \nabla x_k + \frac{1}{p}[(x_k - \omega_k)\nabla p]$$

$$x_k = \frac{\omega_k}{M_k} M, \qquad M = \left(\sum_i \frac{\omega_i}{M_i}\right)^{-1}$$

$\vec{J_i}$ – relative mass flux of specie *i*.

D_{ik} – Fick's diffusion coefficients

$\overrightarrow{d_k}$ – diffusional driving force

x_k – mole fraction of specie k

M_i – molar mass of specie i.

Gases are assumed to obey ideal gas state equation:

$$\rho = \frac{p}{RT} \sum_i x_i M_i$$

Dynamic viscosity of gases were calculated based on molecular kinetic theory[14]:

$$\mu = \sum_i \frac{x_i \mu_i}{\sum_j x_j \phi_{ij}}$$

$$\phi_{ij} = \frac{\left[1 + \left(\frac{\mu_i}{\mu_j}\right)^{\frac{1}{2}} \left(\frac{M_j}{M_i}\right)^{\frac{1}{4}}\right]^2}{\left[8\left(1 + \frac{M_i}{M_j}\right)\right]^{\frac{1}{2}}}$$

Here μ_i is dynamic viscosity of specie *i*.

D. Fluid flow

Dynamics of air and fuel in supply manifolds is governed by Navier-Stokes equations with inertial term:

$$\rho(\vec{u} \cdot \nabla)\vec{u} = \nabla \cdot \left(-p\vec{l} + \mu(\nabla\vec{u} + (\nabla\vec{u})^T) - \frac{2}{3}\mu(\nabla \cdot \vec{u})\vec{l}\right)$$

$$\nabla \cdot (\rho\vec{u}) = 0$$

In the reaction zone and gas distributors one can neglect all dissipative terms except wall friction:

$$\nabla \cdot \left(-p\vec{l}\right) = \mu k^{-1}\vec{u}$$

$$\nabla \cdot \vec{u} = Q_v$$

Here Q_v is density of gas volume generation rate. k is permeability of corresponding virtual media.

RESULTS AND DISCUSSION

A typical temperature distribution is presented on **Fig. 5**. One can observe abrupt increase of airflow temperature at the entrance of air distributor. This is due to high efficiency heat exchange in the shallow air channels of distributor. To confirm this behavior we simulated independently temperature distribution in a single air channel **Fig. 6**.

One can see that the temperature of input airflow equilibrates with the temperature of device within thin layer of 5 mm thickness.

This fact leads us to interesting consequences. It appears that one can lower amount of air needed to cool the stack by lowering temperature of incoming air.

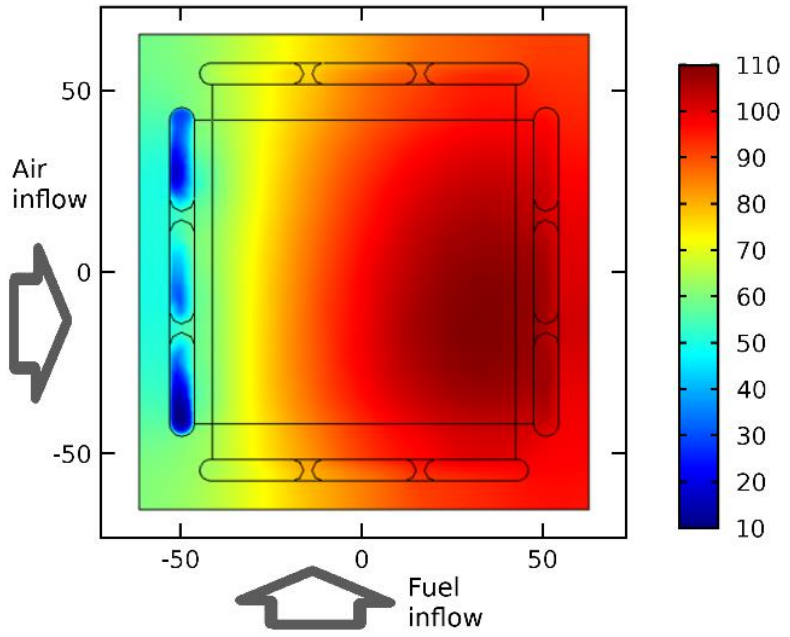

Fig. 5 Temperature (K) distribution in median section of the stack. The reference level is 780 ºC. Voltage of 0.75 V on MEA, current 20 A, fuel utilization 65%. Fuel consists 97% H_2 3% H_2O.

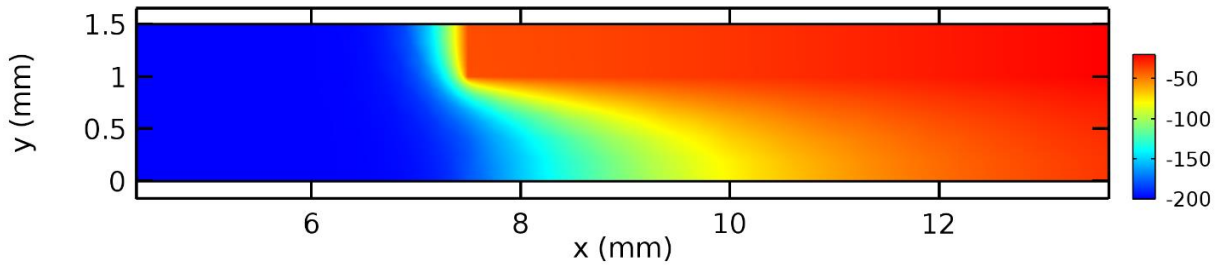

Fig. 6 Temperature distribution in one of the channels of air distributor. Air flows from left to right.

At first sight, lowering the air temperature seems to increase severely temperature gradients across the stack. However, our simulation shows that range of temperature variation inside the stack grows much slower than temperature difference of output and input airflow (**Fig. 7**). Energy losses for air pumping through the stack depend severely on airflow rate (**Fig. 7**). Thus, lowering the temperature of input airflow could help to increase efficiency of the stack.

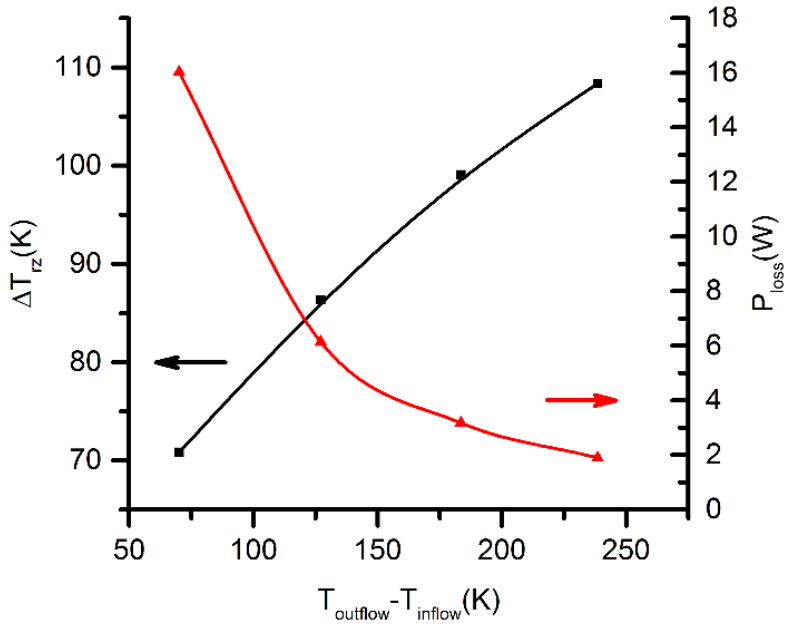

Fig. 7 Dependence of temperature variation range across reaction zone (black squares) and energy losses for pumping air through stack (red squares) on difference of temperature of air outflow and inflow.

On **Fig. 8** we present the amount of energy dissipated by air in the stack on average air velocity in the air supply line. This curve was obtained by variation of the air pipes diameter keeping air inflow rate constant. Red line is inevitable amount of energy needed to overcome viscous wall friction of air in channels of reaction zone and air distributors. One can see that dependence of energy losses is nonlinear **Fig. 8**. This is due to generation of vortices in the input air manifold of stack.

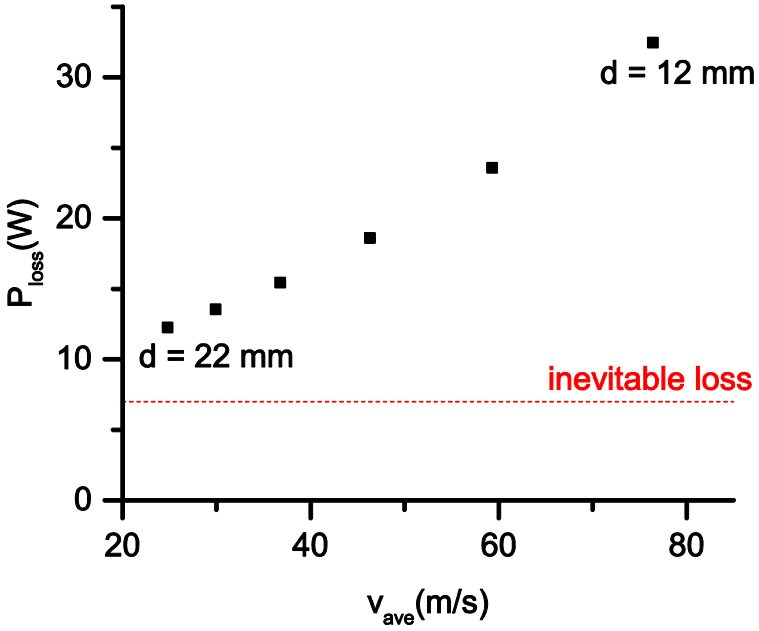

Fig. 8 Dependence of energy losses for pumping air through the stack on the average air velocity in the input air pipe. Here d is the diameter of input air pipe.

Therefore, for the stack efficiency it is important to choose diameter of air supply line large enough. This is important also for the following reason. To distribute reactants uniformly one should provide uniform distribution of air pressure in input and output chambers of stack. Since the variance of pressure is mainly defined by inertia of airflow (see **Fig. 9**) the air velocity should be as low as possible.

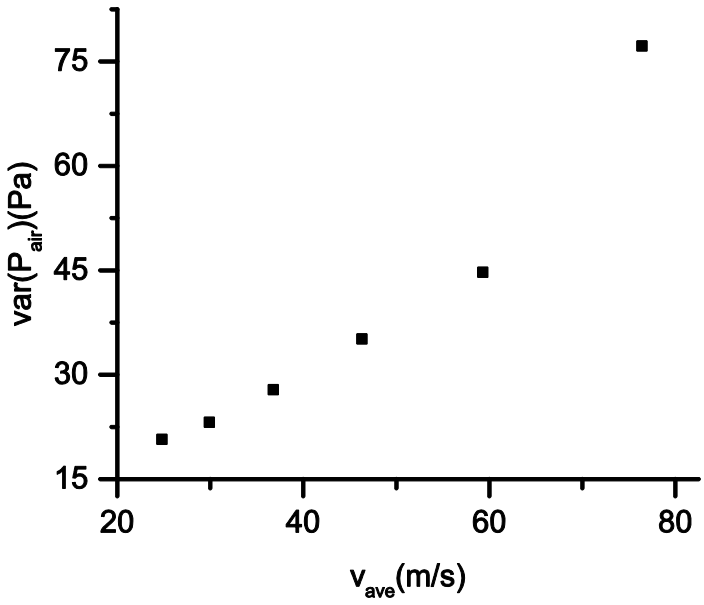

Fig. 9 Dependence of air pressure variation range in the input manifold on the average air velocity in the input air pipe.

CONCLUSIONS

Electrolyte-supported SOFC was prepared in a form of button cell 21 mm in diameter. Series of current-voltage characteristics were measured. Using experimental data a numerical model of SOFC stack was composed. Distributions of temperature, reactants concentrations, gas pressures and velocities were calculated. It is shown that in order to increase efficiency of stack and uniformity of reactants distribution one should increase the diameter of air supply line to suppress vortices generation in the input manifold of the stack. High heat exchange efficiency in the stack gas distribution domains leads to the following effect: dependence of temperature variation amplitude in the reaction zone on temperature of input airflow is weak. The temperature difference over the stack is significantly not equal to the temperature difference between outflow and inflow gases. Depending on the conditions, it may be even 2 times lower. Provided that the stack has certain limitation for the temperature variation this allows one to lower the rate of input airflow thus lowering losses for pumping of air through the stack, compared to the assumption of comparable temperature drops over the solid and gas phases.

Acknowledgements

This work was supported by the Russian Science Foundation grant 17-79-30071 “Scientifically grounded optimization of power and mass-dimensional characteristics of planar SOFC stacks and development of fuel processor for highly-efficient transport and stationary power plants”.

The gas dynamics numerical model of SOFC was developed under financial support of State Task of Institute of Solid State Physics RAS.

REFERENCES

1. Isabella Burch J.G. A Survey on Global Activity to Phase Out Internal Combustion Engine Vehicles, Center for Climate Protection, 2018. https://climateprotection.org/wp-content/uploads/2018/10/Survey-on-Global-Activities-to-Phase-Out-ICE-Vehicles-FINAL-Oct-3-2018.pdf. Accessed 14-May-2019.
2. Tokyo Aims to Realize “Hydrogen Society”by 2020. *We Are Tomodachi.* 2016, vol. 14, pp. 24–25.
3. Minh N.Q., Takahashi T. Science and Technology of Ceramic Fuel Cells. Burlington, Elsevier, 1995, 379 p.
4. Vielstich W., Lamm A., Gasteiger H.A. Handbook of fuel cells. Chichester, Wiley, 2003, 488 p.
5. Bove R., Ubertini S. Modeling solid oxide fuel cells. Great Britain, Springer, 2008, 397 p.
6. Tucker M.C. Progress in metal-supported solid oxide fuel cells: A review. *J. Power Sources.* 2010, vol. 195, pp. 4570–4582.

7. Greco F., Frandsen H.L., Nakajo A., Madsen M.F., van herle J. Modelling the impact of creep on the probability of failure of a solid oxide fuel cell stack. *J. Eur. Ceram. Soc.* 2014, vol. 34, pp. 2695–2704.

8. Bao C., Wang Y., Feng D., Jiang Z., Zhang X. Macroscopic modeling of solid oxide fuel cell (SOFC) and model-based control of SOFC and gas turbine hybrid system. *Prog. Energy Combust. Sci.* 2018, vol. 66, pp. 83–140.

9. Burmistrov I., Agarkov D., Bredikhin S., Nepochatov Y., Tiunova O., Zadorozhnaya O. Multilayered Electrolyte-Supported SOFC Based on NEVZ-Ceramics Membrane. *ECS Trans.* 2013, vol. 57, pp. 917–923.

10. Burmistrov I., Drozhzhin O.A., Istomin S.Y., Sinitsyn V.V., Antipov E.V., Bredikhin S.I. $Sr_{0.75}Y_{0.25}Co_{0.5}Mn_{0.5}O_{3-y}$ Perovskite Cathode for Solid Oxide Fuel Cells. *J. Electrochem. Soc.* 2009, vol. 156, pp. B1212–B1212.

11. Dickinson E.J.F., Ekström H., Fontes E. COMSOL Multiphysics®: Finite element software for electrochemical analysis. A mini-review. *Electrochem. Commun.* 2014, vol. 40, pp. 71–74.

12. Sudaprasert K., Travis R.P., Martinez-Botas R.F. A Study of Temperature Distribution Across a Solid Oxide Fuel Cell Stack. *J. Fuel Cell Sci. Technol.* 2010, vol. 7, p. 11002.

13. Kharton V.V. Solid state electrochemistry. Weinheim, Chichester, Wiley-VCH, 2009-2011, 506 p.

14. Wilke C.R. A Viscosity Equation for Gas Mixtures. *J. Chem. Phys.* 1950, vol. 18, pp. 517–519.

ОПТИМИЗАЦИЯ БАТАРЕИ ТВЕРДООКСИДНЫХ ТОПЛИВНЫХ ЭЛЕМЕНТОВ С ПОМОЩЬЮ МУЛЬТИФИЗИЧЕСКОЙ ЧИСЛЕННОЙ МОДЕЛИ

А.У. Шарафутдинов[1], Ю.С. Федотов[1], С.И. Бредихин[1]

Федеральное государственное бюджетное учреждение науки Институт физики твердого тела Российской академии наук, 142432, Россия, Черноголовка, Московская область, Академика Осипьяна, 2, e-mail: shazat@issp.ac.ru

Мембранно-электродный блок(МЭБ) NiO/10Sc1CeSZ/LSM был изготовлен с помощью технологии трафаретной печати. Был измерен ряд вольт-амперных характеристик. По этим данным была построена численная модель батареи топливных элементов в ПО для конечно-элементных расчетов COMSOL Multiphysics. Были найдены распределения температур, концентраций реагентов, давления и скорости газов. Было обнаружено, что высокая эффективность теплообмена в газораспределительных зонах батареи подавляет зависимость разброса температур в зоне реакции от температуры втекающего в батарею воздуха. Это позволяет понизить количество воздуха, используемого для охлаждения батареи, не увеличивая значительно градиентов температуры в батарее. Также показано, что основной перепад давления воздуха на батарее обусловлен образованием вихрей во входной камере, а не потерями на вязкое трение в зоне реакции батареи.

Ключевые слова: *ТОТЭ, COMSOL, электролит-поддерживающая ячейка, батарея ТОТЭ, вычислительная гидродинамика*